

Interlayer exchange coupling and giant magnetoresistance in Fe/V (001) superlattices

A. Broddefalk, R. Mathieu, and P. Nordblad

Department of Materials Science, Uppsala University, Box 534, SE-751 21, Uppsala, Sweden

P. Blomqvist and R. Wäppling

Department of Physics, Uppsala University, Box 530, SE-751 21, Uppsala, Sweden

J. Lu and E. Olsson

Department of Materials Science, Uppsala University, Box 534, SE-751 21, Uppsala, Sweden

(Received 15 November 2001; revised manuscript received 11 April 2002; published 11 June 2002)

Magnetization and magnetoresistivity studies of Fe/V (001) superlattices are reported. The first giant magnetoresistance peak with respect to the vanadium and iron layer thicknesses is investigated. The interlayer antiferromagnetic coupling strength is found to show a peak at a vanadium layer thickness of 13 atomic monolayers (≈ 20 Å) with a full width at half maximum of about 2 monolayers. The antiferromagnetic coupling shows a maximum at an iron layer thickness of about 6 monolayers (≈ 9 Å) for series of superlattices with vanadium thicknesses around 13 monolayers. The magnitude of the giant magnetoresistance shows a similar variation as the antiferromagnetic coupling strength.

DOI: 10.1103/PhysRevB.65.214430

PACS number(s): 75.70.Pa, 75.70.Cn

I. INTRODUCTION

The interlayer exchange coupling (IEC) of ferromagnetic layers through a nonmagnetic metal has attracted a lot of attention in the last decade, in connection to the giant magnetoresistive (GMR) effect observed in antiferromagnetically coupled layers.^{1,2} This interaction has been shown to oscillate between ferromagnetic (FM) and antiferromagnetic (AF) coupling when varying the spacer layer thickness.³ The IEC has also, both experimentally and theoretically,⁴ been shown to depend on the thickness of the magnetic layers. In this case, the coupling coefficient does not necessarily change sign but may only show a varying magnitude with increasing layer thickness. Similar variations of the GMR ratio with the magnetic layer thicknesses have been reported.¹ Fe/V (iron/vanadium) superlattices have been shown to couple antiferromagnetically for Fe (3 monolayers)/V (12–16 monolayers),⁵ and in a series of Fe(10 Å)/V(t_V), oscillations were found with a maximum in the strength of the antiferromagnetic coupling at V layer thicknesses of $t_V = 22, 32,$ and 42 Å.⁷ One atomic monolayer (ML) of a Fe/V (001) superlattice amounts to about 1.5 Å.

In this paper, the influence of the thickness of the Fe layers on the IEC and the GMR of Fe/V (001) superlattices near the first AF coupling peak ($V \approx 13$ ML) is examined.

II. EXPERIMENT

A. Sample preparation and characterization

The Fe/V superlattices (SL) were grown in a three target magnetron sputtering system with a base pressure of 10^{-10} Torr. The polished MgO (001) substrates ($10 \times 10 \times 0.5$ mm³) were ultrasonically precleaned in ethanol, isopropanol, and acetone before they were outgassed at 800 °C for 30 min. The sputtering gas was Ar with a purity of

99.9999% and the targets used were Fe(99.95%), V(99.7%) and Pd(99.95%). The sputtering gas pressure was 5.0 mTorr and the substrate holder temperature was 400 °C. The sample holder was electrically isolated from ground potential and rotated (~ 30 rpm) during deposition to prevent thickness gradients. The epitaxial relationship between Fe and MgO (001) is Fe [001] \parallel MgO [001] and Fe [110] \parallel MgO [010]. This arrangement gives a nominal lattice mismatch of 3.5%. On the substrate, Fe and V were alternately deposited by using computer-activated shutters. The layer thicknesses were monitored by the deposition time. Typical deposition rates of Fe and V were 0.65 Å/s and 0.45 Å/s respectively. The samples were capped with palladium (Pd) to avoid oxidation. In this paper we use the nomenclature Fe (X ML)/V (Y ML), where X and Y indicate the nominal thicknesses of the Fe and V layers in atomic monolayers, respectively. The Fe thickness ranged from 3 to 13 ML ($X = 3, 5, 6, 9,$ and 13 ML), while V thicknesses ($Y = 11, 12, 13, 14,$ and 15 ML) were chosen around the first AF coupling peak near $Y = 13$ ML.⁵

The structural quality of the SL were investigated by x-ray diffraction (XRD). The measurements were carried out in the low-angle region ($2\theta = 1-20^\circ$) and in the high-angle region ($2\theta = 20-100^\circ$). A Siemens D5000 powder diffractometer was used with the beam defined by 0.3° divergence and receiving slits. For full width at half maximum (FWHM) measurements, the beam was defined by 0.05° slits. The Cu K_α radiation was monochromatized by a secondary graphite monochromator. The SUPREX model was used to determine the Fe/V interface quality.⁶ Table I gives for all SL the number of atomic monolayers and repetitions, the thickness of Pd, as well as the nominal and measured superlattice periods Λ . The nominal Λ is estimated from $\Lambda = X \times a_{Fe}/2 + Y \times a_V/2$, where $a_{Fe} = 2.8664$ Å and $a_V = 3.0274$ Å are the lattice parameters of Fe and V, respectively. The measured Λ value is obtained from the XRD measurements. The error

TABLE I. Data on the Fe (X ML)/V (Y ML) superlattices. Number of atomic monolayers and repetitions, Pd thickness, as well as nominal and measured superlattice period Λ .

Superlattice	Pd (\AA)	Nominal Λ (\AA)	Measured Λ (\AA)
3/11 \times 30	100	20.95	20.80
3/12 \times 30	100	22.46	22.95
3/13 \times 30	100	23.98	24.30
3/14 \times 30	100	25.49	25.85
3/15 \times 30	100	27.00	27.65
5/12 \times 30	100	25.33	25.30
5/13 \times 30	100	26.84	27.00
5/13 \times 30	20	26.84	26.50
5/13 \times 30	0	26.84	26.60
5/14 \times 30	100	28.36	28.25
6/11 \times 30	100	25.25	25.20
6/13 \times 30	100	28.28	28.30
9/11 \times 30	100	29.55	28.35
9/12 \times 30	100	31.06	31.05
9/13 \times 30	100	32.58	32.80
9/14 \times 30	100	34.09	34.15
13/11 \times 30	100	35.28	36.70

on the superlattice period $|\Lambda(\text{nominal}) - \Lambda(\text{measured})|$ is small, and amounts on average to 0.35 \AA , i.e., less than 0.25 ML.

One of the superlattices, Fe (9 ML)/V (13 ML) was characterized by transmission electron microscopy (TEM). A cross-section specimen was prepared by gluing two thin film sample pieces face to face and subsequently cutting slices from the sandwich. Each slice was mechanically ground on both sides to a thickness of $100 \text{ }\mu\text{m}$. The slice was then dimpled to a thickness of $10 \text{ }\mu\text{m}$ at the specimen center whereafter the specimen was ion milled until electron transparency. The TEM analysis was carried out using both a Tecnai F30 ST field-emission gun TEM operated at 300 kV with a Gatan Imaging Filter and a Jeol 2000 FXII TEM operated at 200 kV .

B. Magnetization and magnetoresistance measurements

Hysteresis loops were recorded for all SL at 10 K in a Quantum Design MPMS5 superconducting quantum interference device magnetometer. The magnetic field was applied along the $[100]$ and $[110]$ directions of the Fe layers. The absolute value of the magnetization has been calculated using the total volume of the Fe layers in each SL as the magnetic volume, neglecting any influence from induced moments in the V layers.⁷ For the SL where the coupling was found to be ferromagnetic and an in-plane anisotropy was observed, the anisotropy constant K proportional to the energy difference between the $[110]$ and the $[100]$ direction was deduced from the enclosed area of the two magnetization curves in the first quadrant of the magnetization vs applied field curves. Since the field was applied in plane, where the shape anisotropy is small, no correction of

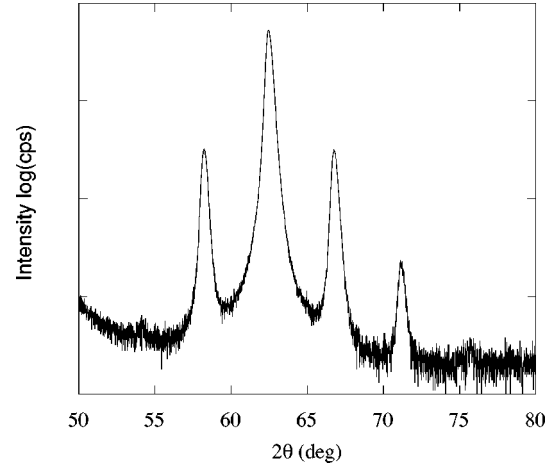


FIG. 1. High-angle x-ray diffraction scan from the Fe (3 ML)/V (13 ML) superlattice. log refers to the natural logarithm.

the field for demagnetization effects was done. For the SL where antiferromagnetic coupling was observed, the coupling strength was estimated from $J = \mu_0 M_s H_{sat} t_{Fe} / 4$, where t_{Fe} is the thickness of the Fe layers and H_{sat} is the saturation field.⁵ Resistivity $\rho(H, T, \theta)$ and magnetoresistance (MR) were measured using a standard four-probe method and a Maglab 2000 system from Oxford Instruments with a rotary probe. The magnetoresistance was recorded in the current-in-plane geometry. θ refers to the angle between the current and the in-plane magnetic field. The resistance was deduced for $H \parallel I (\theta = 0)$ and $H \perp I (\theta = 90^\circ)$ by rotating the sample and always feeding the current between the same contacts. The MR is defined as $\Delta\rho/\rho_0 = (\rho_0 - \rho_{sat})/\rho_0$, with $\rho_0 = \rho(H=0)$ and $\rho_{sat} = \rho(H = H_{sat})$.

III. RESULTS AND DISCUSSION

A high-angle radial scan of the Fe (3 ML)/V (13 ML) superlattice is shown in Fig. 1. The peak at 62.5° is the Fe/V (002) Bragg peak, surrounded by five satellite peaks which originate from the superlattice periodicity. The peaks are sharp and well defined indicating a high structural quality of the sample. The structural coherence length (ζ) in the growth direction can be estimated from the linewidth of the Bragg peak using $\zeta = 1/\Delta q$, where Δq is the linewidth (FWHM in \AA^{-1}) in the radial direction, $q = 2 \sin \theta / \lambda$ is the scattering vector and θ is the angle of the incident and the diffracted x-rays with respect to the sample. An out-of-plane structural coherence length of about 400 \AA was obtained for the Fe (3 ML)/V (13 ML) superlattice. No other peaks than those seen in Fig. 1, were detected in the range $2\theta = 20\text{--}100^\circ$ except reflections from the substrate. Furthermore, a texture scan performed on the Fe (3 ML)/V (13 ML) superlattice showed four (220) peaks separated by 90° indicating a single-crystalline superlattice.

The SUPREX model was used to determine the Fe/V interface roughness. The specular component of the low-angle x-ray diffraction data from the Fe (3 ML)/V (13 ML) super-

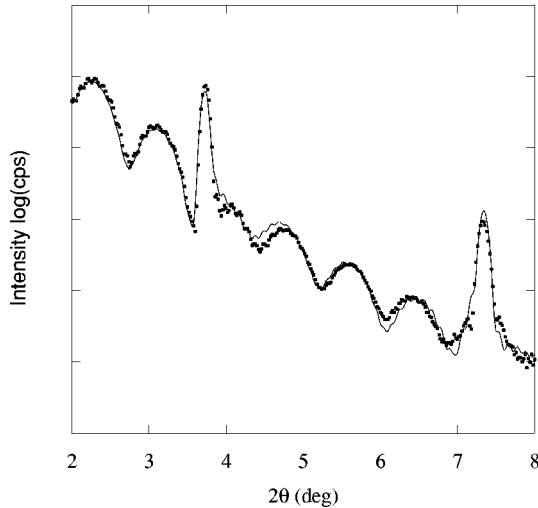


FIG. 2. Low-angle x-ray diffraction scan (specular component) for the Fe (3 ML)/V (13 ML) superlattice. The solid line is the fit to the measured data (filled squares).

lattice in the range $2\theta = 2 - 8^\circ$ is shown in Fig. 2. The result from the fitting procedure is also shown in the figure where two distinct superlattice satellites are clearly visible. The decrease in intensity of the satellites corresponds to an average interface roughness of about two atomic monolayers ($\sim 3 \text{ \AA}$). Furthermore, the results from the fit also indicate that the Fe-on-V (Fe deposited on V) interfaces have a somewhat larger roughness than the V-on-Fe interfaces, a result that is consistent with a recent Mössbauer investigation of the Fe/V interfaces.⁸ It should be pointed out that x-ray diffraction furnishes structural information averaged over length scales corresponding to the coherence length of one photon. In the x-ray diffraction setup that was used, the effective in-plane coherence length of the radiation at low angles is limited by the spectral resolution $\Delta\lambda/\lambda$, to about 1000 \AA . This means that we are measuring random interface roughness as well as correlated roughness induced by the substrate. Reflection high-energy electron diffraction patterns of the Fe and V surfaces indicate a two-dimensional layer by layer growth of both materials.

The TEM micrograph in Fig. 3 shows a cross section of the Fe (9 ML)/V (13 ML) superlattice. The superlattice exhibits flat layers, with no significant thickness fluctuations or waviness. Superlattice satellite reflections are observed around the Fe/V (002) diffraction spot in the selected area electron diffraction (SAED) pattern shown in the figure. It is also evident that the specimen is single crystalline and the epitaxial relationship between the superlattice and the substrate is Fe/V [001] \parallel MgO [001] and Fe/V [110] \parallel MgO [010], as discussed above. A detailed TEM investigation of the interface quality will be further performed.

As exemplified in Fig. 4 (a) for Fe (6 ML)/V (11 ML), the SL with a V layer thickness of 11 monolayers, all showed fourfold in-plane anisotropy, with [100] as the easy axis, except for Fe (3 ML)/V (11 ML), which appeared isotropic inplane. This sample saturated at very low fields, which also excludes AF coupling. The difference in magnetocrystalline

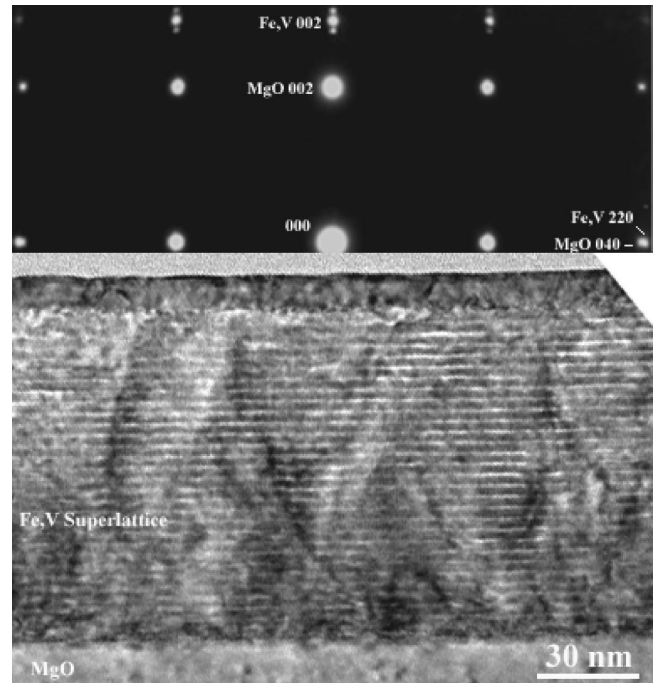


FIG. 3. SAED pattern (top) and TEM micrograph (bottom) of the Fe (9 ML)/V (13 ML) superlattice.

anisotropy energy (E_a) between the [110] and the [100] directions $\Delta E_a = E_a[110] - E_a[100]$, proportional to the anisotropy constant K , increased with the thickness of the magnetic layers. K , however, does not exhibit the $K = K_v + 2K_s/t_{Fe}$ dependence (t_{Fe} is the thickness of the magnetic layers, K_v the volume, and K_s the surface coefficient of the magnetocrystalline anisotropy) that is expected if all SL are equally strained [cf. inset of Fig. 4(a)]. The observed deviations from such a behavior are probably due to the magnetoelastic coupling, since the Fe layers are strained to accommodate a common in-plane lattice parameter with the V layers.⁹⁻¹¹

Fe (3, 6, and 9 ML)/V (13 ML) are magnetically isotropic in plane, but rather large fields are required to reach saturation, implying that the Fe layers are antiferromagnetically coupled. In Fig. 4(b), the magnetization curve for the Fe (6 ML)/V (13 ML) is plotted. The saturation field is considerably larger for the isotropic V (13 ML) SL than for the V (11 ML) SL measured along the hard [110] direction. For a larger Fe thickness, Fe (13 ML)/V (13 ML), the superlattice shows a restored fourfold in-plane anisotropy and the magnetization curves for this sample is very similar to the corresponding curve for the Fe (13 ML)/V (11 ML) SL. This shows that magnetization wise, the AF interlayer coupling has become unresolvably weak for Fe layers in the thickness range 9–13 ML; as seen in the inset of Fig. 4(b), the saturation field of the AF coupled SL drastically decreases when increasing the amount of Fe in the superlattice. The saturation magnetization increases with the number of monolayers of Fe in the samples [cf. Fig. 4(c)].

The magnetic field dependence of the normalized resistivity (ρ/ρ_{sat} or ρ/ρ_0) for the Fe (3, 6, and 9 ML)/V (13 ML) SL, as well as for the Fe (13 ML)/V (11 ML) sample are

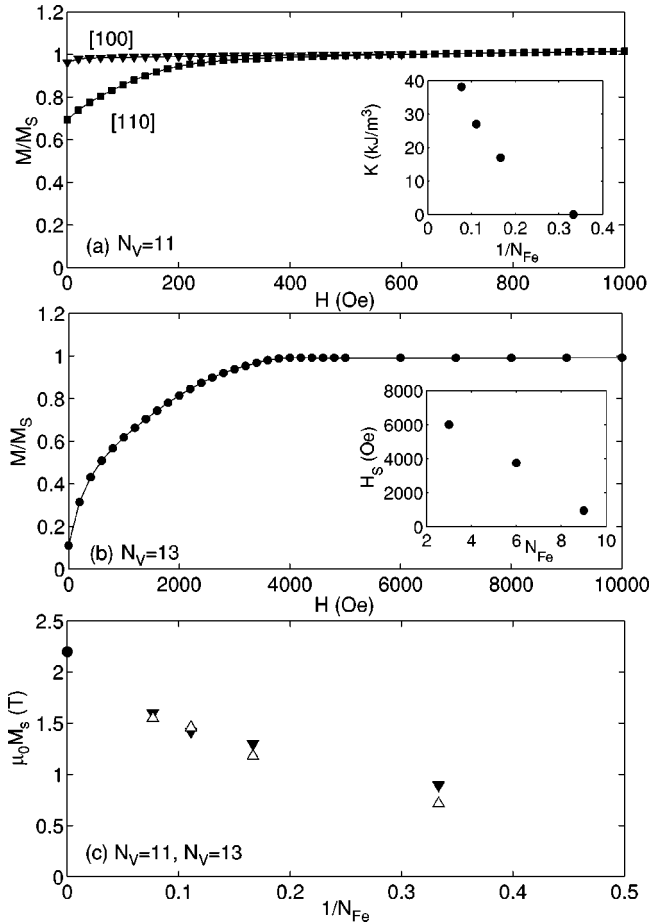


FIG. 4. Magnetization vs magnetic field for (a) Fe (6 ML)/V (11 ML) and (b) Fe (6 ML)/V (13 ML); $T=10$ K. For the FM coupled SL [inset of (a)], the variation of the anisotropy constant K with the inverse of the Fe thickness is included. In the AF case [inset of (b)], the variation of the saturation field is added. In (c) the variation of the saturation magnetization with the inverse of the number of monolayers of Fe is shown; the results for the ferromagnetically coupled superlattices are plotted in filled triangles. The bulk value is added for comparison (filled circle).

shown in Fig. 5(a). GMR is observed for the first three samples, superposed with an increasing anisotropic magnetoresistance (AMR) component of same order of magnitude as for the corresponding sample in the V (11 ML) series. Fe (13 ML)/V (13 ML), on the other hand, displays like Fe (13 ML)/V (11 ML) only AMR features. The saturation fields derived from the GMR curves agree with the corresponding values derived from the magnetization measurements for the SL with thin Fe layers, whereas for the Fe (9 ML)/V (13 ML), a saturation field is clearly seen in the MR behavior but is not resolvable in the magnetization curves. The corresponding value of $\Delta\rho/\rho_0$ for the current Fe (3 ML)/V (13 ML) is lower than a previously reported value⁵ (3% compared to 7%), which could be attributed to the difference in thickness of the capping layer of Pd used, (100 Å compared to 30 Å in the earlier study). The capping layer may affect the coupling strength.¹² The thickness of the capping layer also sets the amount of current going through the superlat-

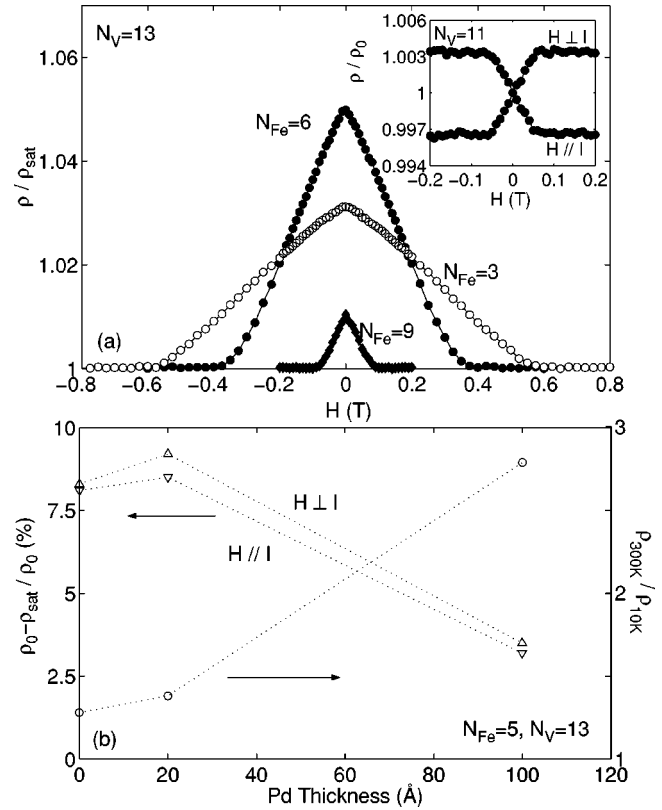


FIG. 5. (a) Magnetoresistance curves for the AF coupled SL (main frame) and for one of the FM coupled SL (inset). (b) illustrates the contribution of the Pd capping layer to the (magneto)resistivity, showing the GMR (right) and resistivity (left) ratios of Fe (5 ML)/V (13 ML) SL with, respectively, 0, 20, and 100 Å of Pd. The dotted lines are guides to the eyes.

tice, which in turn affects the MR ratio. We have observed that the resistivity ratio between 300 K and 10 K [$\rho(300K)/\rho(10K)$] and the magnitude of the measured GMR ratio show a considerable covariation. A larger resistivity ratio yields a lower GMR value for nominally similar Fe/V SL. One obvious reason behind this behavior is as mentioned above, a difference in thickness of the Pd capping layer that we always grow to protect the Fe/V SL from oxidation; in addition, Pd allows the SL to be further processed, facilitating their hydrogenation.¹³ Figure 5(b) shows the effect of this layer on the (magneto)resistivity for an Fe (5 ML)/V (13 ML) SL. Without Pd, or for a small thickness of Pd, the resistivity ratio between room and helium temperatures amounts to ~ 1.3 . It increases by more than a factor of two for ~ 100 Å of Pd. At the same time the magnitude of the GMR effect drops from $\sim 8-9\%$ to $\sim 3\%$. In the following, we will compare the GMR ratios of Fe/V SL having similar zero magnetic field resistivity ratios [$\rho(300K)/\rho(10K) \sim 2$, see inset of Fig. 7]. The SL in the V (11 ML) series show only AMR, as shown in the inset of Fig. 5. The size of $\Delta\rho/\rho_0$ increases with increasing Fe layer thickness, as may be expected from the increased magnetic layer thickness and increasing magnetocrystalline anisotropy.

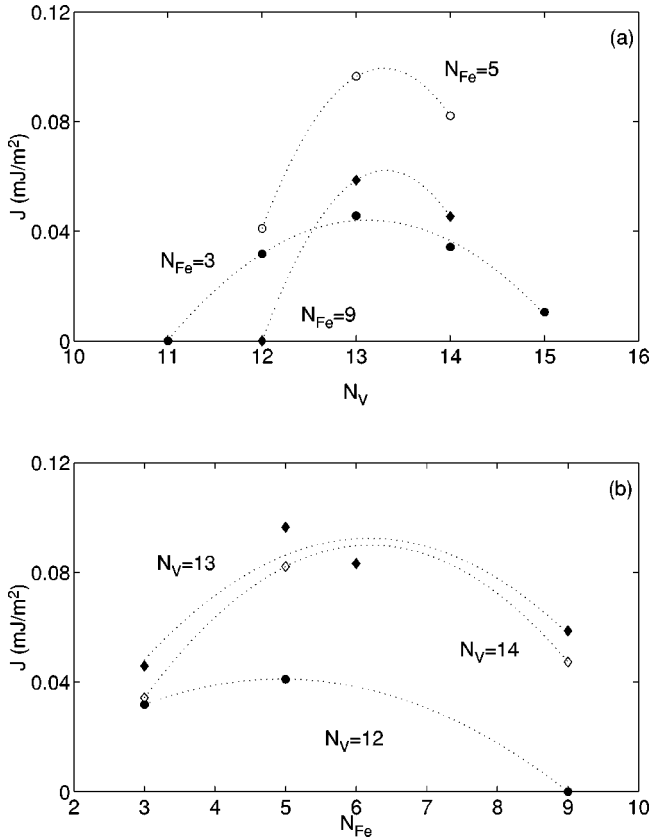


FIG. 6. Coupling strength of the antiferromagnetically coupled SL for (a) varying V thickness and (b) varying Fe thickness. The dotted lines are guides to the eyes.

In Fig. 6(a) the AF interlayer coupling strength is plotted vs the number of V monolayers for SL with 3, 5, and 9 ML of Fe. The three series of Fe/V SL show a maximum of the AF coupling strength at a V thickness of about 13 ML. In Fig. 6 (b), the AF coupling strength is plotted vs the Fe layer thickness for series of SL with V thicknesses of 12, 13 and 14 ML. The AF coupling strength is weaker at a V thickness of 12 ML, but all series of Fe/V SL show similar trends for the dependence of the coupling strength on the Fe thickness, a broad maximum at about 6 ML of Fe may be estimated for all V thicknesses.

The MR values of SL in the V (11 ML) and V (13 ML) series are displayed in Fig. 7. It is worth noting that the two Fe (13 ML) SL show an almost identical behavior only exhibiting an AMR effect. The GMR for the V (13 ML) series shows a maximum of about 5% at an Fe layer thickness of about 6 ML. For the same Fe thickness, the AF coupling strength as well shows a maximum [cf. Fig. 6(b)], which could be related to the oscillatory character of the AF coupling strength with the magnetic layer thickness.¹⁶ The GMR [cf. Fig. 7] and the AF coupling strength [cf. Fig. 6(b)] vanish rapidly when increasing the Fe thickness above 10 ML, and do not seem to reappear for even larger thicknesses.^{10,14} Preliminary results from a study on FeNi/V superlattices¹⁵ indicate a similar behavior. In many other systems, such as Fe/Cr (Ref. 17), Fe/Ti (Ref. 18), or even Co/Cu (Ref. 19), the GMR

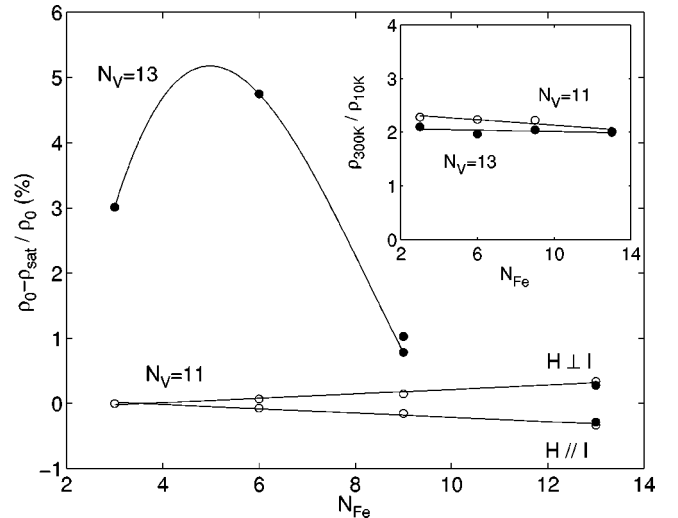


FIG. 7. Magnitude of the GMR and AMR vs N_{Fe} for all SL. The inset shows the corresponding $\rho_{300\text{K}} / \rho_{10\text{K}}$ resistivity ratio.

remains for much larger thicknesses of the magnetic layer. Theoretically,^{16,19,20} the AF coupling (and its oscillations) also remains for relatively larger magnetic layer thicknesses. The superlattice quality remains the same with increasing iron layer thickness, however, due to the lattice mismatch between Fe and V, the in-plane lattice parameter of the body-centered-tetragonal superlattice and the mean out-of-plane lattice parameter decreases somewhat with increasing Fe layer thickness. These changes of the structure influences the electronic structure of V (and Fe) and could possibly change the ability of the V layer to mediate antiferromagnetic coupling.²¹ The rapid disappearance of the AF coupling and the associated GMR in the present set of superlattices will be further discussed in a study of the FeNi/V twin system.

As mentioned above, we have in Fig. 7 only considered the SL showing similar resistivity ratios, as seen in the inset; the GMR values in this plot are thus directly comparable to each other. Of course, differences in the crystalline quality of the films and interfaces may influence the magnitude of the GMR.²²

IV. CONCLUSIONS

The interlayer exchange coupling of Fe/V (001) superlattices shows a first antiferromagnetic maximum at a V thickness of about 13 ML. At a V thickness of 13 ML, the coupling has a maximum strength at an Fe layer thickness of about 6 ML. The magnetoresistance shows GMR effects for the AF coupled SL with a maximum magnitude at the Fe thickness where the AF coupling is largest. It was also found that there is a surprising “cutoff” thickness of the magnetic layer, above which the AF coupling vanishes.

Measurements on a series of Fe/V superlattices with a V thickness of 11 ML showed four fold in-plane anisotropy and

only anisotropic magnetoresistance for all Fe layer thicknesses. An AMR of the same magnitude was seen superposed on the GMR effect for the series of SL with a V thickness of 13 ML.

ACKNOWLEDGMENTS

Financial support from the Swedish Natural Science Research Council (NFR) is acknowledged.

-
- ¹B. Dieny, *J. Magn. Magn. Mater.* **136**, 335 (1994).
²P.M. Levy, *Solid State Phys.* **47**, 367 (1994).
³S.S.P. Parkin, N. More, and K.P. Roche, *Phys. Rev. Lett.* **64**, 2304 (1990).
⁴P. Bruno, *Phys. Rev. B* **52**, 411 (1995); *J. Phys.: Condens. Matter* **11**, 9403 (1999); P.J.H. Bloemen, M.T. Johnson, M.T.H. van de Vorst, R. Coehoorn, J.J. de Vries, R. Jungblut, J. aan de Stegge, A. Reinders and W.J.M. de Jonge, *Phys. Rev. Lett.* **72**, 764 (1994); P. Lang, L. Nordström, K. Wildeberger, R. Zeller, P.H. Dedrichs, and T. Hoshino, *Phys. Rev. B* **53**, 9092 (1996).
⁵P. Granberg, P. Isberg, E.B. Svedberg, B. Hjorvarsson, P. Nordblad, and R. Wäppling, *J. Magn. Magn. Mater.* **186**, 154 (1998).
⁶E.E. Fullerton, I.K. Schuller, H. Vanderstraeten, and Y. Bruynseraede, *Phys. Rev. B* **45**, 9292 (1992).
⁷M.M. Schwickert, R. Coehorn, M.A. Tomaz, E. Mayo, D. Lederman, W.L. O'Brien, Tao Lin, and G.R. Harp, *Phys. Rev. B* **57**, 13 681 (1998).
⁸B. Kalska, P. Blomqvist, L. Häggström, and R. Wäppling, *Europhys. Lett.* **53**, 395 (2001).
⁹É. du Trémolet de Lacheisserie, *Ann. Phys. (Paris)* **5**, 267 (1970); É. du Trémolet de Lacheisserie, *Phys. Rev. B* **51**, 15 925 (1995).
¹⁰P. Granberg, P. Nordblad, P. Isberg, B. Hjorvarsson, and R. Wäppling, *Phys. Rev. B* **54**, 1199 (1996).
¹¹A. Broddefalk, P. Nordblad, P. Blomqvist, P. Isberg, R. Wäppling, O. Le Bacq, and O. Eriksson, *J. Magn. Magn. Mater.* **241**, 260 (2002).
¹²A. Bounouh, P. Beauvillain, P. Bruno, C. Chappert, R. Mégy, and P. Veillet, *Europhys. Lett.* **33**, 315 (1996).
¹³B. Hjorvarsson, J.A. Dura, P. Isberg, T. Watanabe, T.J. Udovic, G. Andersson, and C.F. Majkrzak, *Phys. Rev. Lett.* **79**, 901 (1997).
¹⁴P. Pouloupoulos, P. Isberg, W. Platow, W. Wisny, M. Farle, B. Hjorvarsson and K. Baberschke, *J. Magn. Magn. Mater.* **170**, 57 (1997).
¹⁵B. Hjorvarsson (private communication).
¹⁶P. Bruno, *Europhys. Lett.* **23**, 615 (1993).
¹⁷R. Schad, C.D. Potter, P. Belliën, G. Verbank, V.V. Moshchalkov, and Y. Bruynseraede, *Appl. Phys. Lett.* **64**, 3500 (1994).
¹⁸T. Stobiecki, M. Czapkiewicz, M. Kopcewicz, R. Żuberek and F.J. Castano, *Thin Solid Films* **317**, 306 (1998).
¹⁹S.K.J. Lenczowski, M.A.M. Gijs, J.B. Giesbers, R.J.M. van de Veerdonk, and W.J.M. de Jonge, *Phys. Rev. B* **50**, 9982 (1994).
²⁰See also results on the Fe/Cr system in P.M. Levy, S. Zhang, and A. Fert, *Phys. Rev. Lett.* **65**, 1643 (1990).
²¹O. Le Bacq, O. Eriksson, B. Johansson, P. James, and A. Delin, *Phys. Rev. B* **65**, 134430 (2002).
²²A. Moser, U. Krey, A. Paintner, and B. Zeller, *J. Magn. Magn. Mater.* **183**, 272 (1998).